land

MDPI

Article

A Land Cover Change Detection Approach to Assess the Effectiveness of Conservation Projects: A Study Case on the EU-Funded LIFE Projects in São Miguel Island, Azores (2002–2021)

Rafaela Tiengo [1,2], Silvia Merino-De-Miguel [1], Jéssica Uchôa [2] and Artur Gil [3,*]

[1] Departamento de Ingeniería y Gestión Forestal y Ambiental, ETSIMFMN, Universidad Politécnica de Madrid, 28040 Madrid, Spain; r.dtiengo@alumnos.upm.es (R.T.); silvia.merino@upm.es (S.M.-D.-M.)
[2] cE3c—Centre for Ecology, Evolution and Environmental Changes, Azorean Biodiversity Group, CHANGE—Global Change and Sustainability Institute, University of the Azores, 9500-321 Ponta Delgada, Portugal
[3] IVAR—Research Institute for Volcanology and Risk Assessment, University of the Azores, 9500-321 Ponta Delgada, Portugal
* Correspondence: artur.jf.gil@uac.pt

Abstract: Small oceanic islands, such as São Miguel Island in the Azores (Portugal), face heightened susceptibility to the adverse impacts of climate change, biological invasions, and land cover changes, posing threats to biodiversity and ecosystem functions and services. Over the years, persistent conservation endeavors, notably those supported by the EU LIFE Programme since 2003, have played a pivotal role in alleviating biodiversity decline, particularly in the eastern region of São Miguel Island. This study advocates the application of remote sensing data and techniques to support the management and effective monitoring of LIFE Nature projects with land cover impacts. A land cover change detection approach utilizing Rao's Q diversity index identified and assessed changes from 2002 to 2021 in intervention areas. The study analyzed the changes in LIFE project areas using ASTER, Landsat 8, and Sentinel 2 data through Google Earth Engine on Google Colab (with Python). This methodological approach identified and assessed land cover changes in project intervention areas within defined timelines. This technological integration enhances the potential of remote sensing for near-real-time monitoring of conservation projects, making it possible to assess their land cover impacts and intervention achievements.

Keywords: remote sensing; oceanic islands; Python; Rao's Q; land use; land cover; open data; Google Earth Engine; Google Colab

Citation: Tiengo, R.; Merino-De-Miguel, S.; Uchôa, J.; Gil, A. A Land Cover Change Detection Approach to Assess the Effectiveness of Conservation Projects: A Study Case on the EU-Funded LIFE Projects in São Miguel Island, Azores (2002–2021). *Land* **2024**, *13*, 666. https://doi.org/10.3390/land13050666

Academic Editors: Jingcheng Zhang, Juhua Luo and Rongyuan Liu

Received: 13 April 2024
Revised: 10 May 2024
Accepted: 11 May 2024
Published: 12 May 2024

1. Introduction

Preserving nature and mitigating biodiversity decline have garnered heightened significance, which is evident in expanding protected regions and efforts toward ecological restoration [1]. Small islands, defined as land masses with a total area of less than 10,000 km^2 and a population that does not exceed 500,000 inhabitants, are highly vulnerable to climate change impacts due to a combination of factors, including their remoteness, insularity, limited resources, and exposure to extreme weather events. As a result, small islands require special attention and support to address the unique challenges they face in the context of climate change [2]. Furthermore, small islands face environmental issues directly or indirectly related to land use/land cover changes (LULCCs), such as natural hazards, loss of biodiversity, and proliferation of invasive alien species, some of which are caused by direct human exploitation [3]. In Macaronesian oceanic archipelagos like the Azores, the main threat to nature conservation is LULCCs [4–7]. Nature protection and slowing the rate of biodiversity loss in small oceanic islands have become increasingly essential.

Conservation projects funded by the European Commission under the LIFE Programme (https://cinea.ec.europa.eu/programmes/life_en, accessed on 5 March 2023) assign value to different aspects, namely the preservation of local biodiversity, leisure and tourist value, landscape value, water supply, and scientific and education value [1]. However, identifying and mapping the actions allow to verify the investments in these areas.

The analysis of LULCCs is fundamental for comprehensively understanding and addressing local, regional, and global issues. These encompass a range of phenomena, including alterations in rainfall patterns resulting in droughts [8] and flooding [9], occurrences of landslides [10], coastal erosion [11], the rapid expansion of urban areas [12], intensification of agriculture activity and livestock grazing [13], spreading of invasive alien species [14], and wildfires [15,16], among others.

In recent years, there has been a notable increase in scientific papers focusing on remote sensing (RS) applications in island and coastal regions [17]. This surge underscores the growing recognition of the significance and relevance of such studies within the scientific community and among various stakeholders and decision-makers.

The goal of RS-based change detection (CD) is to discern those areas on digital images that depict a change in the feature of interest between two or more image dates. The reliability of the CD process may be strongly influenced by various environmental factors that might change between image dates [18]. Bitemporal, multitemporal, and time series CD techniques are needed to investigate heterogeneous change types, intensities, and process durations and to suit the various purposes of studies. The era of freely accessible data, in parallel with the growth of non-proprietary toolboxes, should propagate doubly through RS communities and users [19].

In recent years, the RS data processing has primarily relied on conventional workstations, utilizing restricted computational resources. This approach presents significant constraints when dealing with large volumes of data, storage, and analysis, which have changed with the advance of the internet and cloud computing [20].

The convergence of the internet and cloud computing is undeniably revolutionizing the field of science. Using geospatial cloud technologies, such as Google Earth Engine (GEE), scientists can now readily and affordably access vast repositories of geographic information spanning a wide array of subjects. Moreover, it is possible to leverage the computational power offered by cloud computing resources (e.g., Google Colab) to conduct intricate analyses and create detailed maps [21].

Using spectral indices with RS data and techniques is paramount for effectively highlighting LULCC dynamics. Among these indices, the Normalized Difference Vegetation Index (NDVI) is the most widely applied RS-based approach for monitoring vegetation in island and coastal environments [17]. The NDVI is a significant index for identifying LULCCs due to its ability to quantify the density and health of vegetation on small or large spatial scales. By comparing the reflectance of near-infrared and visible red light wavelengths, the NDVI provides insights into vegetation growth, distribution, and health. This index is particularly relevant for LULCC assessments, because it can detect changes in land cover types, such as deforestation, urbanization, or agricultural expansion, by monitoring variations in vegetation cover and condition over time. Additionally, the NDVI serves as a valuable tool for understanding ecosystem dynamics, assessing environmental impacts, and informing land management and conservation strategies [22].

In this context, Rao's Q Index was introduced to address the mathematical limitations observed in the Shannon and Rényi Indices. It considers richness, relative abundance, and pixel values' numerical magnitude and pairwise distance within a multivariate framework. The Rao's Q Index correlates with the total pairwise distances between all pixel values in the analyzed satellite imagery, with each distance being weighted by the relative abundance of the corresponding pixel pairs [23]. This comprehensive approach provides a more nuanced understanding of the data [24]. In environmental studies, Rao's Q Index may constitute a systematic way to identify changes in land cover patterns over time. The index is sensitive to changes even in small areas or where differences are subtle [23] and helps in detecting

alterations in soil and vegetation by quantifying the degree of dissimilarity or similarity between samples taken from different locations or at different times.

The Rao's Q Index has already been used in LULCC studies in different geographic areas (including islands [25]), environmental contexts (e.g., rural areas [26]), natural ecosystems [27], and most widely input was the NDVI [24–26,28–31]. Therefore, this index was applied in this study due to its versatility, making it a valuable tool for understanding landscape dynamics at various scales, including identifying LULCCs.

Taking a step forward, we sought to evaluate the sensitivity of new band combinations to explore the potential of Rao's Q multidimensional approach using the red, green, and short-wave infrared (SWIR 2) spectral bands, not only using the NDVI. The importance of these bands in this research lies in their capability to quantify and visualize vegetation vigor and density, thus providing valuable insights into ecosystem dynamics and land management practices in these sensitive areas.

This paper presents a case study examining LULCCs resulting from the development of EU-funded LIFE projects (2003–2021) on São Miguel Island (Azores Archipelago, Portugal) in the Pico da Vara/Ribeira do Guilherme Special Protection Area, where several ecological restoration actions have been planned, developed, and monitored. This study aims to explore RS-based LULC change detection approaches using Rao's Q Diversity Index to assess the effectiveness of these projects. As far as we know, this paper is the first that employs Rao's Q Index with these band combinations. With this innovative approach, it was possible to identify and monitor the effectiveness of investment LULCCs in EU-LIFE project areas.

2. Materials and Methods

2.1. Study Area

The Azores Archipelago, situated in the North Atlantic Ocean, comprises nine volcanic islands. São Miguel, the largest island within the Azores Archipelago, covers an area of approximately 74,677 hectares and has the highest population, with around 133,000 inhabitants. It is positioned about 1500 km away from mainland Europe, specifically at centroid coordinates X: 632,351.58 m and Y: 4,182,515.23 m in UTM WGS84 26N projection.

The study area is the mountainous region in the eastern part of São Miguel Island (Figure 1), which incorporates the designated Special Protection Area called "Pico da Vara/Ribeira do Guilherme", a Natura 2000 site.

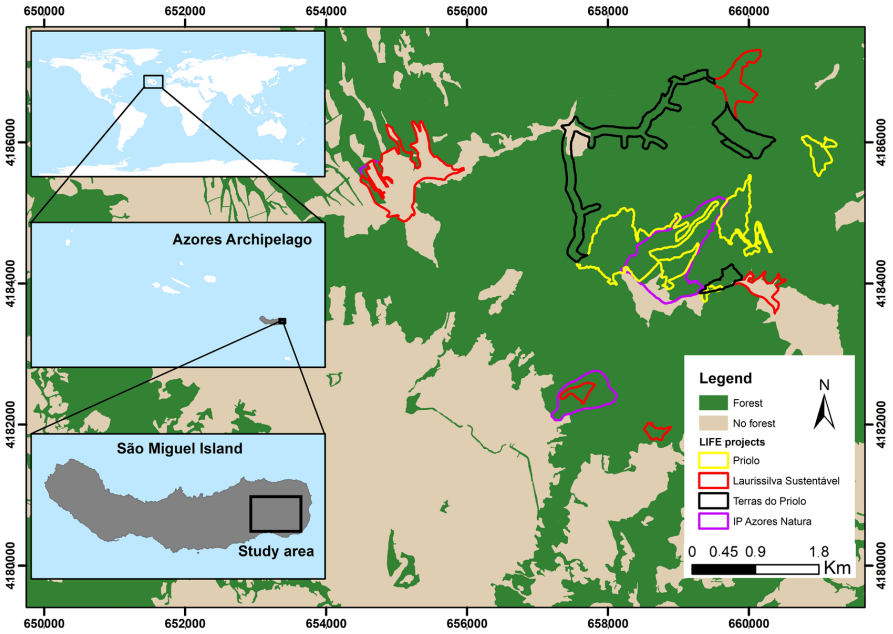

Figure 1. The study area encompasses São Miguel Island, located in the archipelago of the Azores, Portugal, including the areas associated with distinct LIFE projects.

2.2. EU-Funded LIFE Nature Projects in São Miguel Island

The LIFE program was established in 1992 and has since co-financed thousands of projects. LIFE aims to contribute to developing and implementing environmental and climate policy and legislation [32].

Over the years, various LIFE projects have been implemented on São Miguel Island (Figure 2), targeting habitat and species conservation. These projects aimed primarily to conserve and restore the Azores bullfinch (*Pyrrhula murina*) habitat, also known as the Priolo, a critically endangered bird species endemic to the Azores [33].

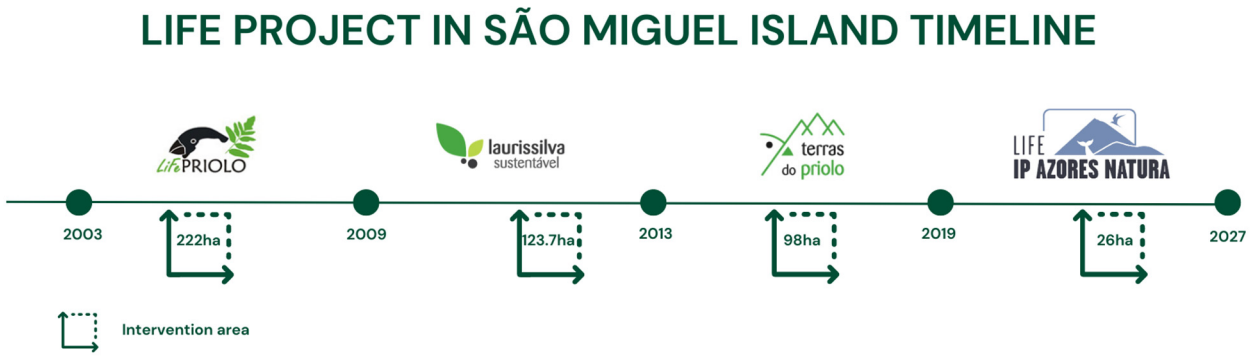

Figure 2. LIFE projects in the São Miguel Island timeline. The first project was LIFE Priolo (October 2003 to November 2008), followed by LIFE Laurissilva Sustentável (January 2009 to June 2013). After this project, the LIFE Terras do Priolo project started (July 2013 to June 2019), and the ongoing project is the LIFE IP Azores Natura (January 2019 to December 2027) [33–37].

The Priolo, a bird species exclusive to the eastern region of São Miguel Island in the Azores, faced a critical endangerment status, ranking as the most threatened bird and the second-rarest in Europe. Its status on the IUCN Red List of Threatened Species was revised in December 2016 and updated to "Vulnerable" according to BirdLife International (https://www.iucnredlist.org/species/22720676/205920049, accessed on 9 June 2023), with the update from "Critically Endangered" to "Endangered" taking place in 2010 [35]. The Priolo population ranges from 500 to 800 breeding pairs, showing a gradual population growth pattern, and occupies a distribution area of 36.5 km^2 [38]. The primary threat to its survival stems from its habitat's substantial and alarming degradation over time. This natural Laurisilva forest habitat remains in very remote areas of São Miguel Island. Furthermore, invasive plant species such as *Myrica faya*, *Pittosporum undulatum*, and *Clethra arborea* pose severe risks to the survival of the native vegetation [33].

2.3. Challenges of Satellite Remote Sensing of Islands

RS enables data collection about our planet's surface using distant tools (e.g., satellites, unmanned aerial vehicles, and airplanes). This technique is especially valuable for isolated island regions, where conventional on-the-ground data gathering is often problematic due to their remote and complex location. With RS, scientists and practitioners can obtain a detailed understanding of an island's landscape. However, there are certain drawbacks to leveraging this method for island territories. The detailed nuances of island environments may go unnoticed due to the spatial capabilities of some sensors. Moreover, not all sensors have the spectral capacity to identify unique characteristics specific to these territories. One notable obstacle is the persistent cloudiness hanging over numerous islands, hindering data collection [39].

Cloud coverage poses significant challenges to obtaining operational satellite imagery of small oceanic islands. Clouds can significantly degrade the quality and reduce the quantity of satellite imagery available for the area of interest. Thick cloud cover can completely obscure the surface, while even thin or scattered clouds introduce shadows, distortions, and reduced contrast in the images. These factors affect the interpretability and accuracy of the data obtained.

Small oceanic islands, such as São Miguel, frequently experience overcast conditions for extended periods, making it challenging to find suitable time windows to capture cloud-free images. This limitation impacts the temporal resolution of satellite imagery, hindering the effective monitoring of changes over time, such as vegetation growth, urban development, or environmental changes on the islands [39].

The geographical positioning of our study area is on the highest mountainous part of São Miguel Island, which often correlates with an increased cloud cover. Due to this, the manual selection of satellite images is usually needed. The manual selection allows researchers to meticulously identify images less affected by cloud cover, ensuring the accuracy and reliability of the data obtained.

2.4. Methodological Workflow

The present study is grounded in a Python code developed for a Rao's Q-based agricultural land cover change detection application [26] (available at https://github.com/AndreaTassi23/spectralrao-monitoring, accessed on 1 March 2023). Adopting the code from [26] as our starting point, we aimed to harness its foundational structure and expand and adapt its functionalities. It was done by integrating improvements and introducing new features in response to our investigation's emergent demands and needs.

This research utilized Google Colab with GEE integration, employing Python as the programming language in a stepwise manner: (1) accessing the satellite imagery repository (including ASTER, Landsat 8 (L8), and Sentinel-2 (S2) sensors) on the GEE catalog; (2) extracting the red, green, near-infrared (NIR), and SWIR 2 bands of the imagery and calculating the NDVI; (3) calculating the Rao's Q classic [15] using the NDVI; (4) calculating Rao's Q multidimensional (MD 1, MD 2, and MD 3); (5) calculating the square root of the post-image minus the pre-image for each project duration; (6) calculating the threshold; and (7) validation of the results through statistical analysis for each LIFE project, complemented by information from reports and historical high-resolution images obtained from satellites (Figure 3).

The GEE (https://earthengine.google.com/, accessed on 7 April 2023) is a cloud-based geospatial data analysis platform that allows users to access and analyze large-scale, multidimensional satellite imagery and other geospatial data [40]. This allows users to access and control the data efficiently, perform rapid prototyping, and visualize the results [40–43].

Throughout these LIFE projects (2002 to 2021), we utilized a progression of satellite sensors, starting with ASTER, followed by L8, and ultimately transitioning to S2.

For the ASTER imagery, the "ASTER/AST_L1T_003" data collection was used (https://developers.google.com/earth-engine/datasets/catalog/ASTER_AST_L1T_003, accessed on 13 June 2023). For the L8 imagery, the "LANDSAT/LC08/C02/T1_L2" data collection was used (https://developers.google.com/earth-engine/datasets/catalog/LANDSAT_LC08_C02_T1_L2, accessed on 13 June 2023). For the S2 imagery, the "COPERNICUS/S2_SR_HARMONIZED" collection was utilized (https://developers.google.com/earth-engine/datasets/catalog/sentinel-2, accessed on 22 May 2023).

Despite the inherent constraints of the GEE, particularly regarding the maximum number of pixels that can be accessed concurrently, the platform offers many significant advantages. Foremost, the GEE provides swift and efficient access to an extensive repository of satellite images, which markedly enhances spatial analysis processes.

However, when dealing with areas that exceed 262,144 pixels, downloading data in the raster file format becomes necessary. Recognizing the significance of a refined and seamless user experience, we devised an automated solution for images up to 262,144 pixels. This innovation ensures that users swiftly acquire the desired images for areas that do not surpass the aforementioned pixel count.

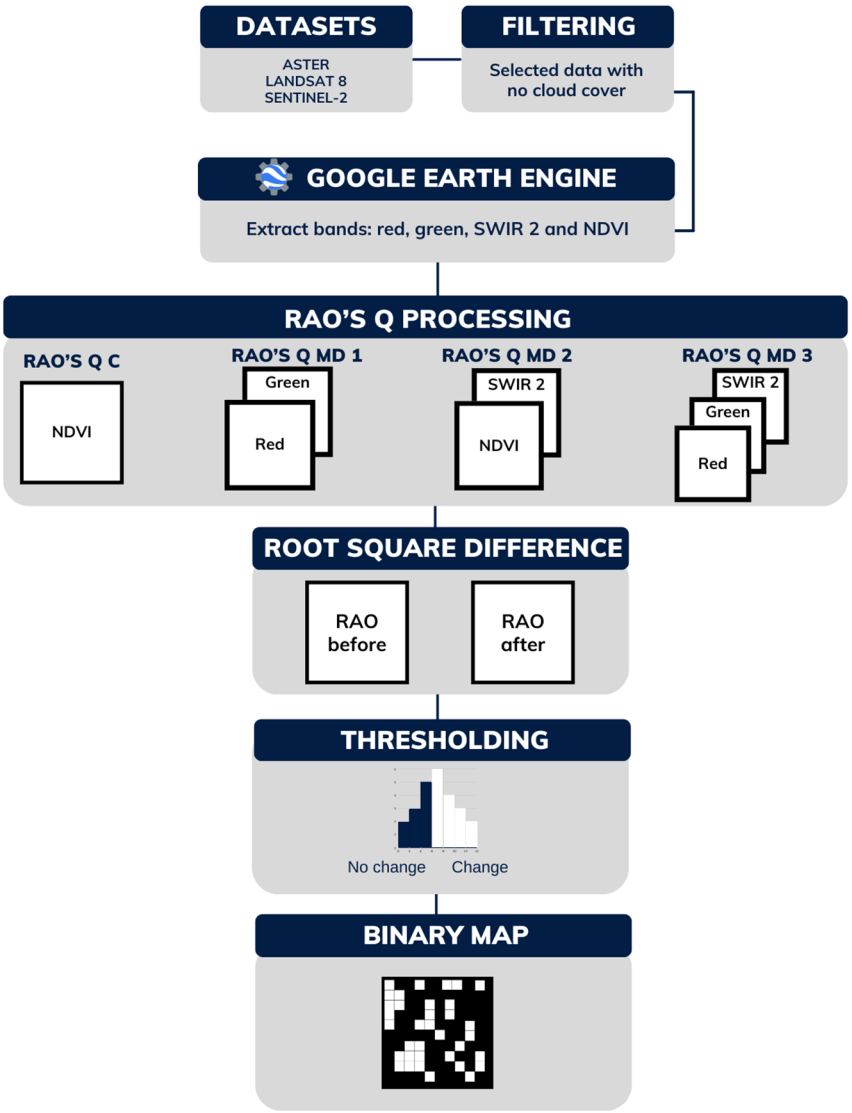

Figure 3. A schematic diagram illustrating the general workflow used to calculate the heterogeneity (Rao's Q) for each LIFE project (2003–2021). MD 1 used the green and red bands for ASTER, L8, and S2. MD 2 used the SWIR 2 and NDVI bands for L8 and S2. MD 3 used the red, green, and SWIR 2 bands for L8 and S2.

2.4.1. NDVI Processing

The NDVI [44] of the RS imagery was calculated before and after each LIFE project intervention. The NDVI is a prevalent index extensively adopted to estimate the vegetation vigor and heterogeneity and consequently identify eventual LULCCs [17]. The mathematical representation for the NDVI is provided by Equation (1):

$$NDVI = \frac{NIR - Red}{NIR + Red} \quad (1)$$

This index is critical in ecological and agricultural studies [45–47], aiding in monitoring changes in vegetation over time and across different landscapes [48], including identifying alterations such as vegetation removal [49] or changes in vegetative vigor [50].

2.4.2. Calculating Rao's Q Index

As described by Rocchini [51], Rao's Q is a quantitative measure used to assess the similarity or dissimilarity between spatial patterns or distributions of ecological variables.

Rao's Q was determined by using a fixed window size of 9 × 9 pixels, selected for index retrieval [23,51]. The formula to calculate the Rao's Q Index was used according to [29]:

$$Rao's\ Q = \sum d_{ij} \times p_i \times p_j$$

In this context, d_{ij} represents the spectral separation between pixel i and j, while p_i signifies the proportion of pixel i relative to others within a window of $n \times n$ pixels (i.e., $p_i = \frac{1}{n^2}$).

The open-source repository created and developed for this research was named "Raoq_GEE" and is accessible on GitHub at https://github.com/rafaelatiengo/Raoq_GEE. Users can locate the Python-implemented methods within the repository to reproduce the research results.

Defining the study area can be accomplished within the code by specifying geographic coordinates or drawing the polygon of interest directly on the map. This approach offers considerable flexibility in data processing, catering to different types of usage and various strategies that future users may adopt. Such versatility facilitates code customization to meet a range of needs and specific applications, enabling the greater adaptability and utility of the system. It is also possible to add shapefiles of the study area if the users have the area on their device in vector format.

The difference among each pair of Rao's Q maps (e.g., RaoC_2014-2010 or RaoC_2015-2020) is determined by the pixel values associated with the estimated change intensity [26] using Equation (2).

$$Root\ Square\ Difference = \sqrt{\left(Rao_{After} - Rao_{Before}\right)^2} \quad (2)$$

Rao's Q classic NDVI was calculated across various temporal intervals corresponding to each LIFE project development. Concurrently, according to spectral data availability, the multidimensional Rao's Q Index was computed in one mode for ASTER (MD 1) and three modes for L8 and S2 (MD 1, MD 2, and MD 3)—see Table 1.

Table 1. Combination of bands used to calculate Rao's Q with the different sensors.

Rao's Q Classic (ASTER, L8, and S2)	Rao's Q MD 1 (ASTER, L8, and S2)	Rao's Q MD 2 (L8 and S2)	Rao's Q MD 3 (L8 and S2)
NDVI	Red + Green	NDVI + SWIR2	Red + Green + SWIR 2

These different methods (classical, MD 1, MD 2, and MD 3) were calculated in order to demonstrate the performance of Rao using different band combinations. To compare the results, the vegetation index most widely applied in island environments (NDVI) [17] was used in the classic mode.

We sought to test whether other combinations of bands would have good accuracy in identifying LULCCs, as different combinations of bands (and sometimes combined with the NDVI, as in MD 2) can demonstrate different results for the same area. The bands chosen for the composition of the different processes (red, green, and SWIR 2) were chosen based on (i) the availability of sensor bands and (ii) the sensitivity of the bands to vegetation/change detection.

With this methodology's capability to identify and assess heterogeneity, it becomes feasible to detect regions where changes occurred within the project sites and the timeframe during which these underwent interventions.

2.4.3. Threshold-Based Change Detection

The dissimilarity between each pair of Rao's Q maps (before and after) is represented by pixel values indicative of change intensity estimates. Following each methodological approach (classic, MD 1, MD 2, and MD 3), a definitive binary map featuring "change" and

"no change" classes was generated using a threshold value. The optimal threshold value was determined by identifying the maximum perpendicular line intersecting the secant line between the highest and lowest points of the histogram. This criterion ensures that only significant changes beyond normal variations are identified, contributing to the accuracy of the CD process [26]. Figure 4 is an example of how the threshold is determined.

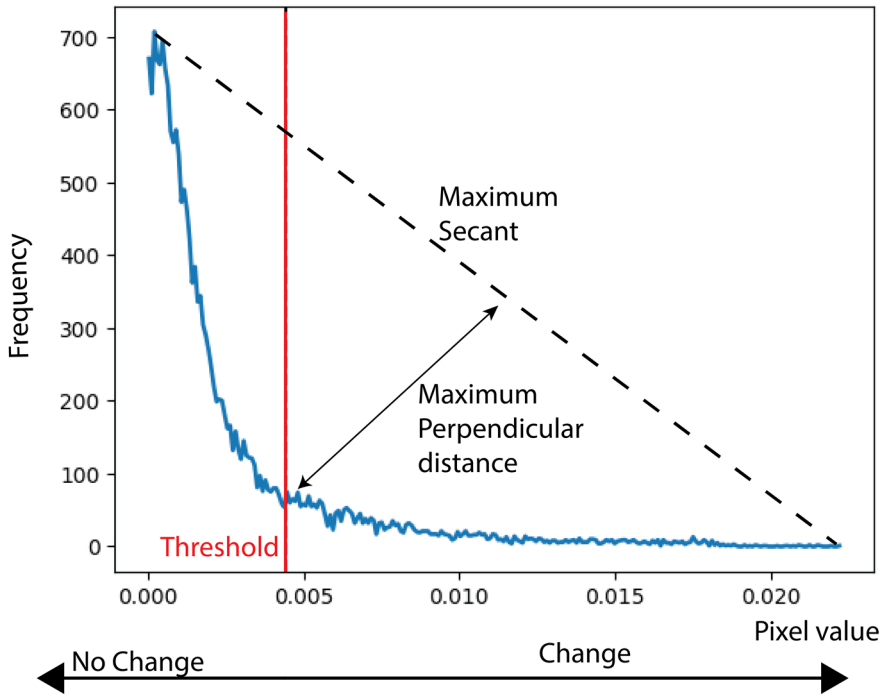

Figure 4. Histogram depicting the threshold secant determination exemplified with Sentinel 2 images (2018–2021).

2.4.4. Overall Accuracy Assessment

To evaluate the accuracy of the several Rao's Q-based approaches in generating binary maps (referred to as C, MD 1, MD 2, and MD 3), we calculated the overall accuracy (OA) in percentage (%) of a correct classification [52]. This procedure involved generating and analyzing 100 random points individually created using QGIS 3.10, with 50 points classified as change and 50 indicating no change for each case study (LIFE project). Each classified point was analyzed and assessed as correctly/incorrectly classified through a GIS-based photo interpretation of very high-resolution orthophotomaps and satellite imagery (e.g., Google Earth), supported by each project's monitoring reports.

The parameters to classify the values in these categories were based on the methods' accuracy classification as low agreement (below 40), moderate agreement (41 to 60), good agreement (61 to 75), excellent agreement (76 to 80), and almost perfect agreement (above 80) [17,53–55].

3. Results

During the different LIFE projects developed on the island of São Miguel since 2003, not all project areas underwent direct interventions in land cover. In this work, only areas of LIFE projects with direct interventions in land cover (ecological restoration and control/eradication of invasive alien species actions) were analyzed, leaving aside interventions unrelated to land cover (e.g., rodent control and the creation of greenhouses and nurseries).

3.1. Priolo Project (2003–2008)

Throughout the Priolo project, extensive removal of invasive alien plant species (e.g., *Clethra arborea* and *Hedychium gardnerianum*) occurred across vast areas [56]. By consulting the false color composite in Figure 5, changes in the area before and after the interventions conducted by the *Sociedade Portuguesa para o Estudo das Aves* (SPEA) become apparent.

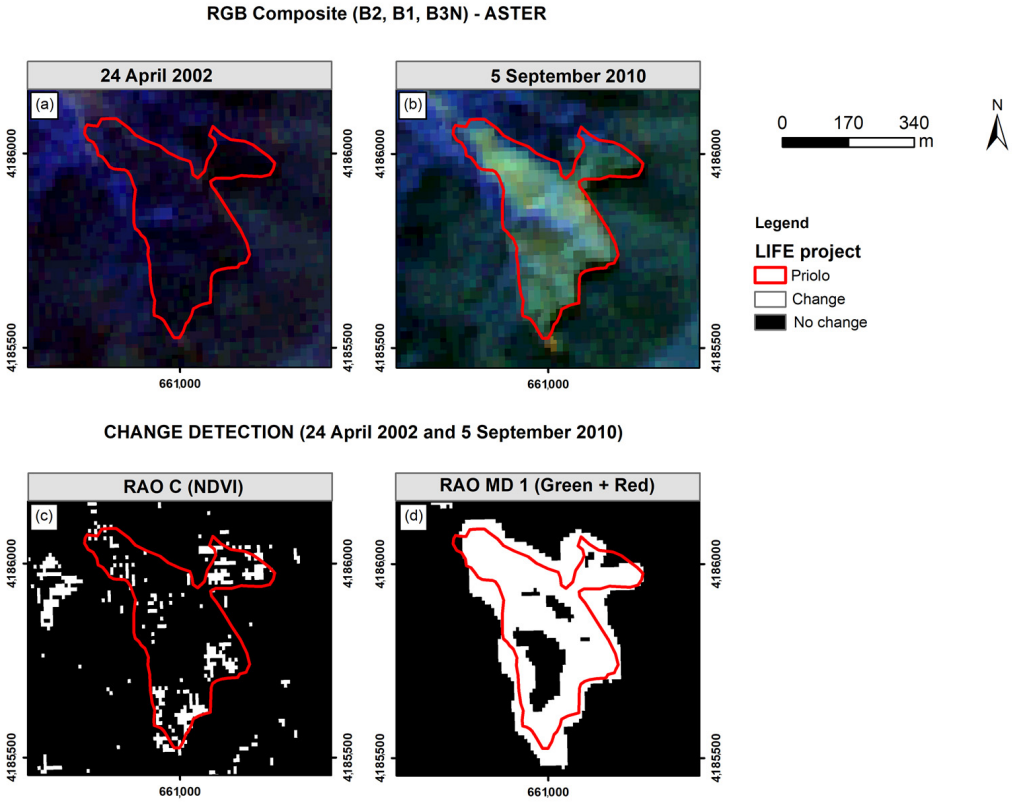

Figure 5. Priolo project area intervened: ASTER false color composite of before (**a**) and after (**b**) the interventions implemented in the area as part of the LIFE Priolo project. Comparison between change detection with Classic Rao's Q Index using the NDVI (**c**) and multidimensional Rao's Q (MD 1) using green and red bands (**d**). Images from the ASTER sensor dated 24 April 2002 and 5 September 2010 were used.

The classic Rao's Q with the NDVI (Figure 5c) could not identify a relevant portion of the area with clearcutting (the primary intervention carried out), presenting an OA of 62 (good agreement) nevertheless. In areas with high rainfall and humidity levels, like the Azores, vegetation reestablishes its vegetative vigor very quickly, which can influence the results obtained using the vegetation index alone.

Rao's Q MD 1 (Figure 5d) showed the best results in identifying the vast intervention area by the Priolo project, with an OA showing an almost perfect agreement (83).

3.2. Laurissilva Sustentável Project (2009–2013)

Several actions were carried out during the Laurissilva Sustentável project at the "Mata dos Bispos" area. Examining the false color composite comprehensively depicts the LULCC before and after the interventions (Figure 6).

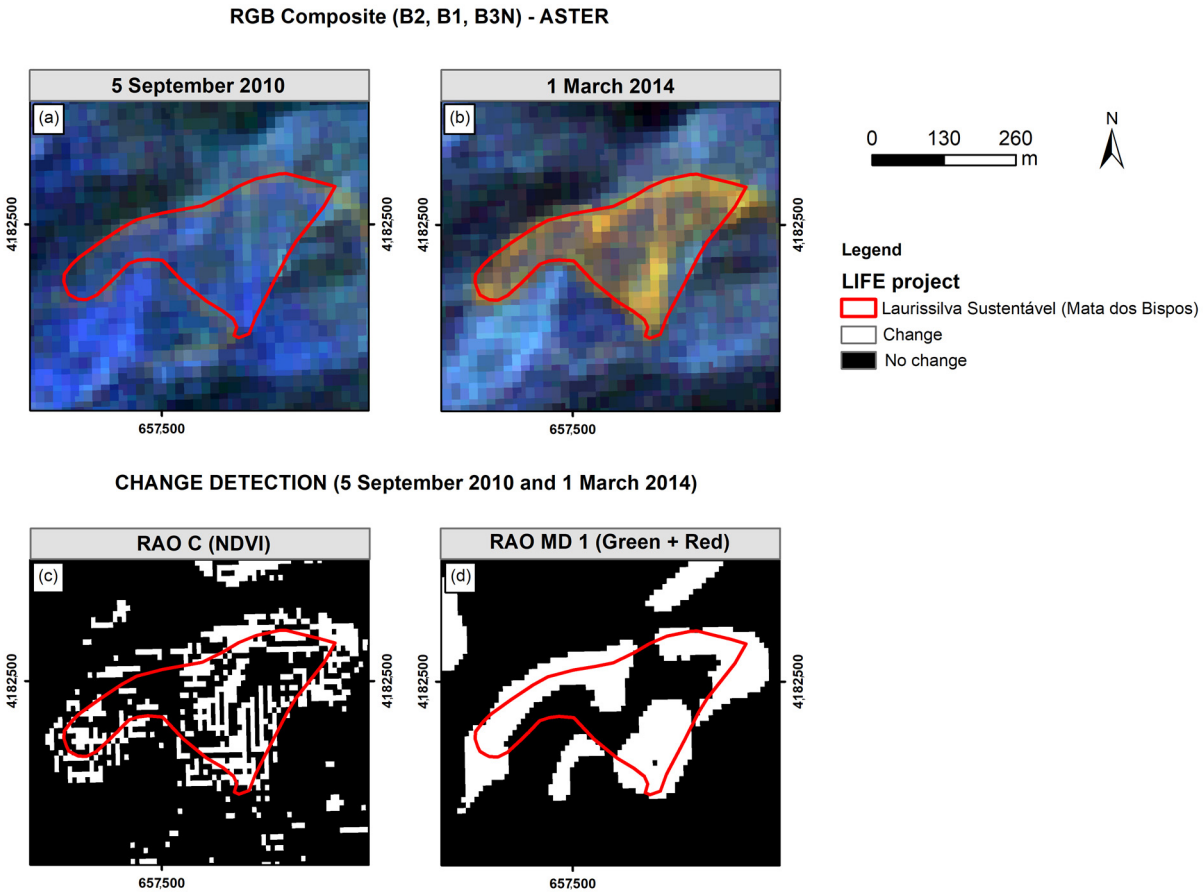

Figure 6. Laurissilva Sustentável project area intervened: ASTER false color composite of before (**a**) and after (**b**) the interventions implemented in the area. Comparison between change detection with the classic Rao's Q Index using the NDVI (**c**) and multidimensional Rao's Q (MD 1) using green and red bands (**d**). Images from the ASTER sensor dated 5 September 2010 and 1 March 2014 were used.

In this area, the classic Rao's Q with the NDVI (Figure 6c) proved a good agreement (OA: 73), demonstrating robust results in identifying areas affected by interventions during the execution of the Laurissilva Sustentável project.

Rao's Q MD 1 (Figrue 6d) showed more promising and accurate results with excellent agreement (OA: 79), effectively identifying an extensive and continuous area affected by changes.

3.3. Terras do Priolo Project (2013–2019)

The Terras do Priolo project's intervention area was in the core area of the "Pico da Vara/Ribeira do Guilherme" Special Protection Area. Before the intervention, this area was dominated by dense patches of alien invasive plant species.

According to the project report, the activities commenced in 2016 at lower elevations within a *Pittosporum undulatum* invaded area where a clearcutting was carried out.

Following this action, 1.4 hectares of *Pittosporum undulatum* patches along the Ribeira do Guilherme water stream banks were intervened. Due to the steep slopes in that area and the impossibility of removing vegetative debris that could endanger the flow of the stream, the girdling technique was employed in this area [35].

In the areas above 450 m, characterized by forests dominated by native and endemic species, an intervention to control *Hedychium gardnerianum* patches was conducted. The girdling technique was applied for the two invasive tree species (*Clethra arborea* and *Pittosporum undulatum*) [35].

In total, 26 hectares were intervened in this area, establishing an altitudinal gradient of native vegetation ranging from 300 to 900 m. For further details regarding this action, please refer to Figure 7.

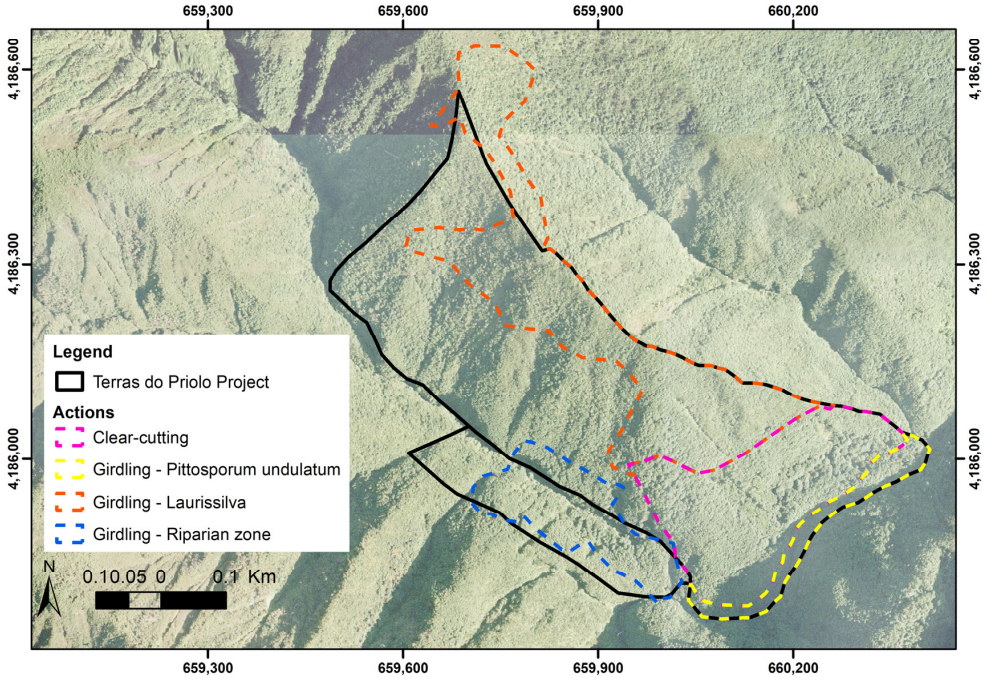

Figure 7. Types of interventions carried out during the Terras do Priolo project [35].

Analyzing the L8-derived false color composite, it depicts the comprehensive changes in land cover before and after interventions in the designated Terras do Priolo project area (Figure 8).

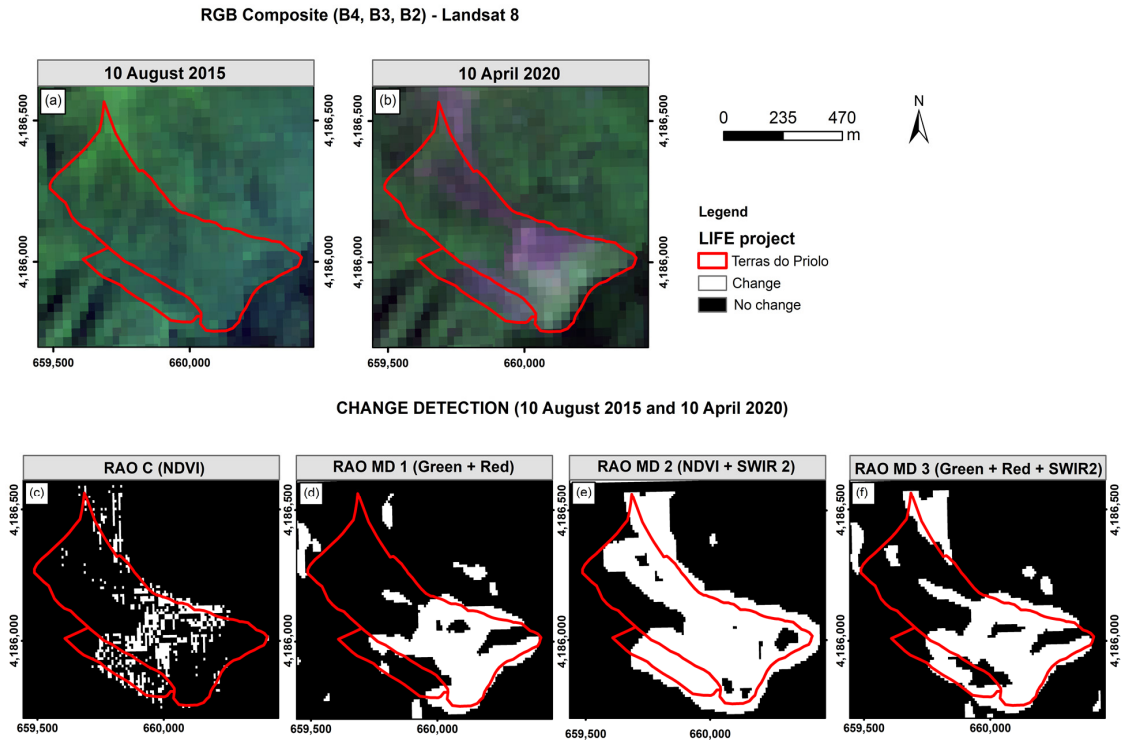

Figure 8. Terras do Priolo project area intervened: L8 false color composite of before (**a**) and after (**b**) the interventions implemented in the area as part of the LIFE Terras do Priolo project. Comparison

between change detection with classic Rao's Q Index using the NDVI (**c**); multidimensional Rao's Q 1 (MD 1) using green and red bands (**d**); multidimensional Rao's Q 2 (MD 2) using the NDVI and SWIR 2 band (**e**); and multidimensional Rao's Q 3 (MD 3) using green, red, and SWIR 2 bands (**f**). Images from the L8 sensor dated 10 August 2015 and 10 April 2020 were used.

Rao's Q classic with the NDVI (Figure 8c) identified LULCCs with a good agreement (OA: 64). Rao's Q MD 1 (Figure 8d) showed slightly better accuracy (OA: 74) by detecting mainly the clearcut area previously unidentified by classic Rao's Q with the NDVI. Rao's Q MD 2 (Figure 8e) was highly effective in identifying the most altered areas with an almost perfect agreement (OA: 94), including the subarea where *Pittosporum undulatum* girdling interventions were carried out. This result demonstrates that Rao's Q MD 2 can effectively detect changes in areas with mixed interventions. In contrast, Rao's Q MD 3 approach (Figure 8f) showed similar results to Rao's Q MD 1, with an OA of 74 (good agreement).

3.4. IP Azores Natura Project (2019–2027)

The IP Azores Natura project was initiated in 2019, including an intervention area that was previously intervened under the Laurissilva Sustentável project.

When analyzing the S2-based false color composite from December 2018 (Figure 9a), it is possible to observe the regeneration of vegetation that occurred in the intervened area of the Laurissilva Sustentável project, which concluded in 2013. In the March 2021 false color composite, it is also possible to observe the first interventions carried out in the LIFE IP Azores Natura's intervention area.

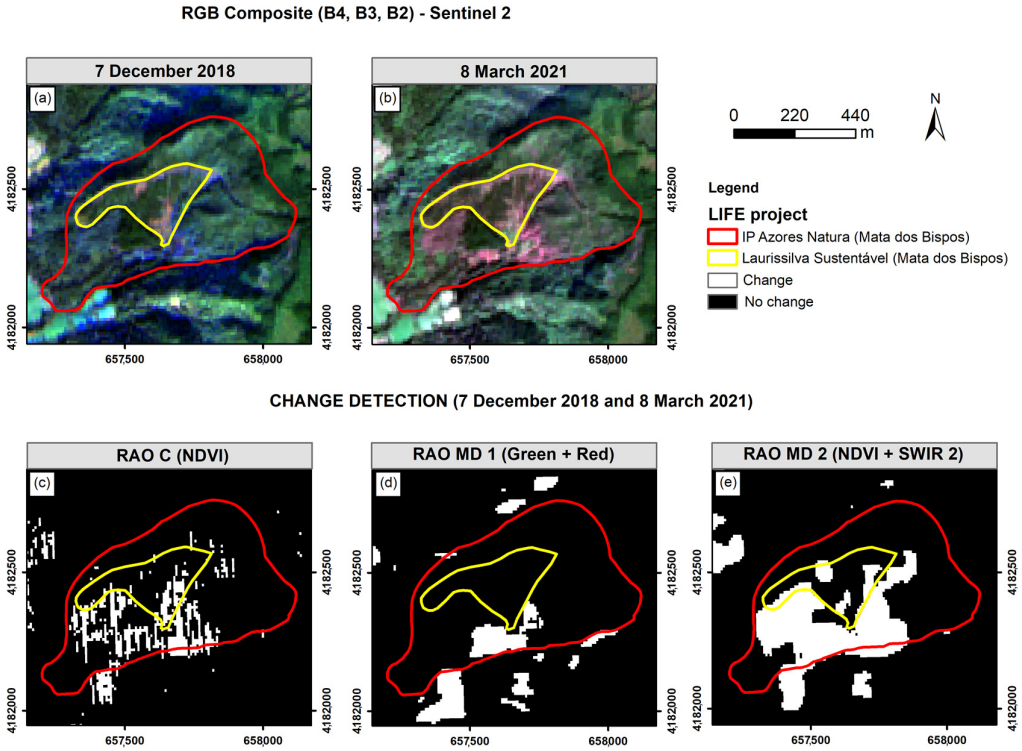

Figure 9. IP Azores Natura project area intervened: S2-based false color composite of before (**a**) and after (**b**) the initial interventions implemented in the area as part of the LIFE IP Azores Natura project. Comparison between change detection with classic Rao's Q Index using the NDVI (**c**); multidimensional Rao's Q 1 (MD 1) using green and red bands (**d**); multidimensional Rao's Q 2 (MD 2) using the NDVI and SWIR 2 band (**e**); and multidimensional Rao's Q 3 (MD 3) using green, red, and SWIR 2 bands (**f**). Images from the S2 sensor dated 7 December 2018 and 8 March 2021 were used.

The intervention area in the LIFE IP Azores Natura project covers the entire upper section of "Ribeira dos Bispos". The density of patches dominated by *Pittosporum undulatum* has emerged as the most concerning issue in this area, and, therefore, the priority was to control this species initially to prevent its spread. An area of 29.3 hectares of *Pittosporum undulatum* has been intervened using the girdling technique, employing herbicide injection. In total, an additional 4.5 hectares were intervened in an area dominated by the native species *Myrica faya* and the alien invasive species *Clethra arborea*. The interventions targeted the understory through chemical control, aiming to prevent the reinvasion of areas subsequently restored by the project. In the riparian zone, a strip of 10 m along watercourses was intervened, involving the permanent removal of alien invasive plants. An area of 1.1 hectares, dominated by *Myrica faya, Clethra arborea,* and *Pittosporum undulatum*, was intervened using chemical control and girdling techniques [36]. This project is underway until 2027, and its operational plan states that specific interventions will apply the girdling technique in this area.

Classic Rao's Q analysis using the NDVI (Figure 9c) revealed almost perfect agreement results (OA: 88) in detecting and identifying the most relevant project-driven LULCCs. Nevertheless, Rao's Q MD 1 (Figure 9d) could not identify the most altered areas, showing a moderate agreement (OA: 60). Rao's Q MD 2 (Figrue 9e) showed the best results for this case study using S2 spectral bands (OA: 91), while Rao's Q MD 3 (Figure 9f) showed limited effectiveness in identifying LULCCs, with an OA of 68 (good agreement).

3.5. Overall Accuracy Assessment

Table 2 shows the OA results for the Rao's Q-based methodological approaches. Overall, the approach showing the best results was Rao's Q MD 2, illustrating a high potential to identify project-driven land cover changes.

Table 2. Overall accuracy results for each Rao's Q methodological approach.

Study Area (Sensor)	Rao's Q Classic (NDVI)	Rao's Q MD 1 (Green + Red)	Rao's Q MD 2 (NDVI + SWIR2)	Rao's Q MD 3 (Green + Red + SWIR2)
Priolo (ASTER)	62	83		
Laurissilva Sustentável (ASTER)	73	79		
Terras do Priolo (L8)	64	74	94	74
IP Azores Natura (S2)	88	60	91	68

4. Discussion

This research focused on identifying land cover changes driven by the development of EU-funded LIFE conservation projects on S. Miguel Island (Azores Archipelago, Portugal) since 2003 to assess the effectiveness of their ecological restoration and invasive alien plant species control and eradication activities.

This research employed several remote sensing-based approaches applying Rao's Q Diversity Index (in its classic and multidimensional forms) to spectral indices (NDVI) and combinations of spectral bands (green, red, and SWIR 2) from open satellite data: ASTER (Priolo and Laurissilva Sustentável projects), L8 (Terras do Priolo project), and S2 (IP Azores Natura project) sensors.

The results from different sensors and band combinations were analyzed. Regarding the results obtained using ASTER data (Priolo and Laurissilva Sustentável projects), the application of classic Rao's Q with the NDVI showed good agreement (OA = 62 and 73). Nevertheless, excellent agreement (OA = 79) and almost perfect agreement (OA = 83) were performed when applying Rao's Q MD1 approach (with green and red spectral bands) utilizing green and red bands in conjunction with processing (MD 1). The lack of quality (due to topographic and atmospheric effects) of the available ASTER's NIR bands necessary to compute the NDVI might explain these better results without the NDVI. Although there is low seasonality throughout the year in the case study area due to the altitudinal gradient

(high altitude, mountainous topography, and high humidity all year), the fact that both pairs of ASTER images were caught in different months (April/September for Priolo and September/March for Laurissilva Sustentável) might also affect negatively the accuracy of the results. Furthermore, it was impossible to compute Rao's Q MD 2 approach (NDVI and SWIR 2) due to the absence of ASTER's SWIR data since April 2008.

Concerning the results obtained using L8 data (Terras do Priolo project), classic Rao's Q using the NDVI; Rao's Q MD 1 (using green and red spectral bands); and Rao's Q MD 3 (using green, red, and SWIR 2 spectral bands) showed only a good agreement (OA = 64, 74, and 74, respectively). In contrast, Rao's Q MD 2 (using the NDVI and SWIR 2) showed an almost perfect agreement (OA = 94). This project's area had different types of field interventions. The classic Rao's Q using the NDVI showed more aptitude for detecting changes in girdling areas. Rao's Q MD1 and Rao's Q MD 3 presented more responsiveness in clearcutting areas. The constant high humidity implies a quick recovery of vegetation, which could explain the higher difficulty in identifying land cover changes when using only the NDVI. Nevertheless, the integration of SWIR spectral bands has been recognized in previous studies [57–59] for the high capability to improve discerning vegetation patterns, especially in areas with shadows due to topography, as in our study area. Although there is low seasonality throughout the year in the case study area due to the altitudinal gradient, the fact that the pair of L8 images analyzed were caught in different months (August/April) might also negatively affect the results' accuracy. Despite the lower spatial resolution of L8 imagery (30 m), the excellent results obtained with Rao's Q MD 2 (using the NDVI and SWIR 2), which was able to detect both girdling and clearcutting areas, demonstrate that the correct combination of high-quality spectral data can somehow mitigate its lower spatial resolution impacts in larger intervention areas.

Regarding the results achieved using the S2 sensor applied to the IP Azores Natura project assessment, classic Rao's Q using the NDVI and Rao's Q MD 2 (using the NDVI and SWIR 2 bands) established an almost perfect agreement (OA = 88 and 91, respectively). As occurred with the previous L8-based case study, combining the NDVI and SWIR2 spectral bands was the most reliable and accurate approach to detect land cover changes in the intervention area. In contrast, Rao's Q MD 1 (with green and red bands) demonstrated moderate agreement (OA = 60), and Rao's Q MD 3 (using green, red, and SWIR 2 bands) exhibited only good agreement (OA = 68). Both approaches could not detect some of the most relevant changes in the intervention area. Although there is low seasonality throughout the year in the case study area due to the altitudinal gradient, the fact that the pair of S2 images analyzed were caught in different months (December/March) might also negatively affect the results' accuracy. Nevertheless, these results show that the high spatial resolution (10 m) of the S2 data constitutes a significant advantage in implementing this methodological monitoring approach of conservation projects implying land cover changes.

Numerous studies have effectively applied Rao's Q Index to analyze LULCC patterns from satellite-derived data. Our research aligns with prior investigations. For instance, Tassi et al. [26] achieved a classification accuracy of 0.91 using Rao's Q classic method with the NDVI, while our study attained 88 accuracy using Rao's Q classic with the NDVI derived from Sentinel-2 imagery.

Similarly, Tassi et al. [26] reported an accuracy of 0.88 when employing Rao's Q in multidimensional mode, whereas our investigation achieved a higher accuracy rate of 94 in the same mode.

Our findings are in accordance with previous studies, such as the work conducted by Khare et al. [24] and Liccari et al. [28], who utilized NDVI data as input for estimating Rao's Q diversity.

One of the main limitations was the limited availability of satellite images for the study areas due to cloud cover, a recurring issue in oceanic islands. Additionally, the study areas were located at the highest part of the island, further increasing the difficulty of obtaining high-quality images. Another limiting factor was the fact that the ASTER sensor's SWIR stopped functioning, preventing a direct comparison to the results obtained

using the SWIR 2 from L8 and S2, which showed better outcomes. Moreover, the use of free sensors with different spatial resolutions may have impacted the comparative results between the sensors.

In summary, for these case studies, the ideal land cover change monitoring approach using open satellite data would be operated by using Rao's Q MD 2 with S2-based NDVI and SWIR 2 data captured during the same season of the year (despite the low meteorological and physiographical variability in the study areas). As previously explained, the low historical and chronicle availability of open satellite data (especially L8 and S2) for this study area is due mainly to cloud cover and significantly restricts its use for operational and management purposes. Therefore, the use of commercial very high spatial and temporal resolution satellite data with good spectral resolution (e.g., available SWIR bands) such as the Worldview-3 mission (https://www.satimagingcorp.com/satellite-sensors/worldview-3/, accessed on 9 March 2024) might provide a cost-effective solution to overcome most technical limitations on the use of the methodological approaches presented in this research in well-funded conservation projects such as the EU-LIFE Programme. The same reasoning can be applied to commercial UAV-based solutions offering very high spatial resolution, unlimited temporal resolution (revisiting time depending only on fieldwork planning), and good spectral resolution (VNIR + SWIR sensors).

This methodology has proven to be an effective tool for analyzing and quantifying changes in land over time, especially on small islands. The limits used to assess accuracy are indicated in the reports as intervention areas. In this sense, the present study made it possible to confirm the interventions carried out. As a result, Rao's Q Index has become a fundamental component in assessing and monitoring land dynamics, significantly contributing as a powerful tool to remotely monitor the EU-LIFE investments and actions during and after the projects.

5. Conclusions

This study presented a methodology for monitoring actions during and after EU-funded LIFE conservation projects on S. Miguel Island, Portugal. This demonstrated the potential to identify whether actions were unrolled in accordance with planned strategies and reported activities, serving as a method of verifying the utilization of financial investments.

The methodology extended the spectral analyses of Rao's Q Index with new band combinations. The use of the SWIR band minimized the impacts of shadows and atmospheric attenuation in the satellite images, thereby enhancing the identification of intervened areas in conjunction with the NDVI. This facilitated the identification of a greater number of interventions (e.g., clearcutting and girdling), capitalizing on the sensitivities of different wavelengths.

The results from the ASTER, Landsat 8, and Sentinel 2 sensors were analyzed. Multidimensional approaches with the NDVI and SWIR 2 bands showed the highest agreement in detecting changes. However, seasonal differences in image acquisition affected the results.

Overall, the ideal approach for LULCC monitoring would involve using S2-based NDVI and SWIR 2 data captured during the same season of the year. However, the limited availability of open satellite data due to cloud cover necessitates exploring commercial very high spatial and temporal resolution satellite data or UAV-based solutions for the effective monitoring of conservation projects such as the EU-LIFE Programme.

Therefore, this research represents a significant advancement in using RS techniques, specifically Rao's Q Index, for monitoring and assessing the development and achievements of conservation projects with land cover implications like those funded by the EU-LIFE Programme. This monitoring approach might be implemented from different perspectives by scientists, conservation managers/practitioners, funding agencies, and further stakeholders to increase ecological restoration activities' cost-effectiveness.

This study also sets the stage for further exploring and developing alternative Rao's Q-based methodological approaches, encouraging future research to explore novel combinations of bands, spectral indices, and sensors. Such advancements are crucial for refining

methodologies in ecological monitoring and land cover dynamics analysis, particularly in island ecosystems where conservation efforts are paramount. Furthermore, we encourage future studies to test this methodology in different geographic areas and ecosystems, expanding its applicability and robustness beyond island ecosystems, thus contributing to the refinement of methodologies for monitoring and analyzing land cover dynamics on a global scale.

Author Contributions: Conceptualization, R.T. and A.G.; methodology, R.T. and J.U.; code, R.T. and J.U.; validation, R.T. and J.U.; data curation, R.T. and J.U.; writing—original draft preparation, R.T.; writing—review and editing, A.G. and S.M.-D.-M.; supervision, A.G. and S.M.-D.-M. All authors have read and agreed to the published version of the manuscript.

Funding: This research was partially funded by the SMILES COST Action, grant number CA21158, by financing a Short-Term Scientific Mission (STSM) of the first author, Tiengo R., at the Polytechnic University of Madrid.

Institutional Review Board Statement: Not applicable.

Data Availability Statement: The open-source repository created and developed for this research was named "Raoq_GEE" and is accessible on GitHub at https://github.com/rafaelatiengo/Raoq_GEE. Users can locate the Python-implemented methods within the repository to reproduce the research results.

Acknowledgments: The authors gratefully acknowledge Andrea Tassi for developing and freely providing in his GitHub repository (https://github.com/AndreaTassi23/spectralrao-monitoring) the Rao's Q-based agricultural LULCC detection operational framework and for the additional information and materials shared. The authors gratefully acknowledge the GIS information and technical reports shared by SPEA—Sociedade Portuguesa para o Estudo das Aves, namely Rui Botelho, Tarso Costa, Azucena de La Cruz, Filipe Figueiredo, and also João Torres (former staff member). The first author, Rafaela Tiengo, gratefully acknowledges the Group of Earth Observation for Quantitative Biosphere Dynamics (Polytechnic University of Madrid, Spain), especially its coordinator, Alicia Palacios-Orueta, and also Diego Madruga Ramos for their support during the process of building and automating the Python code.

Conflicts of Interest: The authors declare no conflicts of interest. The funders had no role in the study's design; in the collection, analyses, or interpretation of the data; in the writing of the manuscript; or in the decision to publish the results.

References

1. Chape, S.; Harrison, J.; Spalding, M.; Lysenko, I. Measuring the Extent and Effectiveness of Protected Areas as an Indicator for Meeting Global Biodiversity Targets. *Philos. Trans. R. Soc.* **2005**, *360*, 443–455. [CrossRef]
2. Rietbergen, S.; Hammond, T.; Sayegh, C.; Hesselink, F.; Mooney, K. *Island Voices-Island Choices Developing Strategies for Living with Rapid Ecosystem Change in Small Islands World Headquarters International Union for Conservation of Nature Ecosystem Management Series No. 6*; IUCN: Gland, Switzerland, 2008.
3. Massetti, A.; Gil, A. Mapping and Assessing Land Cover/Land Use and Aboveground Carbon Stocks Rapid Changes in Small Oceanic Islands' Terrestrial Ecosystems: A Case Study of Madeira Island, Portugal (2009–2011). *Remote Sens. Environ.* **2020**, *239*, 111625. [CrossRef]
4. Gil, A.; Fonseca, C.; Benedicto-Royuela, J. Land Cover Trade-offs in Small Oceanic Islands: A Temporal Analysis of Pico Island, Azores. *Land Degrad. Dev.* **2018**, *29*, 349–360. [CrossRef]
5. Thunig, H.; Wolf, N.; Naumann, S.; Siegmund, A.; Jurgens, C.; Uysal, C.; Maktav, D. Land Use/Land Cover Classification for Applied Urban Planning—The Challenge of Automation. In Proceedings of the 2011 Joint Urban Remote Sensing Event, Munich, Germany, 11–13 April 2011; IEEE: Piscataway, NJ, USA, 2011; pp. 229–232.
6. Bhandari, A.; Joshi, R.; Thapa, M.S.; Sharma, R.P.; Rauniyar, S.K. Land Cover Change and Its Impact in Crop Yield: A Case Study from Western Nepal. *Sci. World J.* **2022**, *2022*, 5129423. [CrossRef]
7. Setiawan, C.; Muzani, M.; Warnadi, W.; A'Rachman, F.R.; Qismaraga, Q. Analysis of Land Cover Changes after the Eruption of Mount Sinabung Using Satellite Imagery. *J. Phys. Conf. Ser.* **2019**, *1402*, 022108. [CrossRef]
8. Zhao, Y.; Zhang, J.; Bai, Y.; Zhang, S.; Yang, S.; Henchiri, M.; Seka, A.M.; Nanzad, L. Drought Monitoring and Performance Evaluation Based on Machine Learning Fusion of Multi-Source Remote Sensing Drought Factors. *Remote Sens.* **2022**, *14*, 6398. [CrossRef]

9. Shastry, A.; Carter, E.; Coltin, B.; Sleeter, R.; McMichael, S.; Eggleston, J. Mapping Floods from Remote Sensing Data and Quantifying the Effects of Surface Obstruction by Clouds and Vegetation. *Remote Sens. Environ.* **2023**, *291*, 113556. [CrossRef]
10. Casagli, N.; Intrieri, E.; Tofani, V.; Gigli, G.; Raspini, F. Landslide Detection, Monitoring and Prediction with Remote-Sensing Techniques. *Nat. Rev. Earth Environ.* **2023**, *4*, 51–64. [CrossRef]
11. Causon Deguara, J.; Gauci, R.; Inkpen, R. Monitoring Coastal Erosion Using Remote Images: Comparison between Physically and Remotely Acquired Data on a Limestone Coast. *Remote Sens.* **2022**, *15*, 36. [CrossRef]
12. Forget, Y.; Shimoni, M.; Gilbert, M.; Linard, C. Mapping 20 Years of Urban Expansion in 45 Urban Areas of Sub-Saharan Africa. *Remote Sens.* **2021**, *13*, 525. [CrossRef]
13. Fernandes, J.P.; Guiomar, N.; Gil, A. Strategies for Conservation Planning and Management of Terrestrial Ecosystems in Small Islands (Exemplified for the Macaronesian Islands). *Environ. Sci. Policy* **2015**, *51*, 1–22. [CrossRef]
14. Costa, H.; Bettencourt, M.J.; Silva, C.M.N.; Teodósio, J.; Gil, A.; Silva, L. *Invasive Alien Plants in the Azorean Protected Areas: Invasion Status and Mitigation Actions*; Springer: Berlin/Heidelberg, Germany, 2013.
15. Zhao, Y.; Huang, Y.; Sun, X.; Dong, G.; Li, Y.; Ma, M. Forest Fire Mapping Using Multi-Source Remote Sensing Data: A Case Study in Chongqing. *Remote Sens.* **2023**, *15*, 2323. [CrossRef]
16. Achour, H.; Toujani, A.; Trabelsi, H.; Jaouadi, W. Evaluation and Comparison of Sentinel-2 MSI, Landsat 8 OLI, and EFFIS Data for Forest Fires Mapping. Illustrations from the Summer 2017 Fires in Tunisia. *Geocarto Int.* **2022**, *37*, 7021–7040. [CrossRef]
17. Tiengo, R.; Palácios-Orueta, A.; Uchôa, J.; Gil, A. Remote Sensing Approaches for Land Use/Land Cover Change in Coastal Areas and Oceanic Islands: An Open Science-Based Systematic Review. *Rev. Gestão Costeira Integr.* **2023**, *23*, 155–177. [CrossRef]
18. Mishra, S.; Shrivastava, P.; Dhurvey, P. Change Detection Techniques in Remote Sensing. *J. Adv. Inf. Technol. Converg.* **2016**, *6*, 51. [CrossRef]
19. Panuju, D.R.; Paull, D.J.; Griffin, A.L. Change Detection Techniques Based on Multispectral Images for Investigating Land Cover Dynamics. *Remote Sens.* **2020**, *12*, 1781. [CrossRef]
20. Mishra, S.; Shrivastava, P.; Dhurvey, P. Change Detection Techniques in Remote Sensing: A Review. *Int. J. Wirel. Mob. Commun. Ind. Syst.* **2017**, *4*, 1–8. [CrossRef]
21. Wright, D.; Harder, C. *GIS for Science: Applying Mapping and Spatial Analytics*, 1st ed.; Esri Press: Redlands, CA, USA, 2019; Volume 1.
22. Bannari, A.; Morin, D.; Bonn, F.; Huete, A.R. A Review of Vegetation Indices. *Remote Sens. Rev.* **1995**, *13*, 95–120. [CrossRef]
23. Rocchini, D.; Marcantonio, M.; Da Re, D.; Bacaro, G.; Feoli, E.; Foody, G. From Zero to Infinity: Minimum to Maximum Diversity of the Planet by Spatio-Parametric Rao's Quadratic Entropy. *Glob. Ecol. Biogeogr.* **2021**, *30*, 1153–1162. [CrossRef]
24. Khare, S.; Latifi, H.; Rossi, S. A 15-Year Spatio-Temporal Analysis of Plant β-Diversity Using Landsat Time Series Derived Rao's Q Index. *Ecol. Indic.* **2021**, *121*, 107105. [CrossRef]
25. Tassi, A.; Gil, A. A Low-Cost Sentinel-2 Data and Rao's Q Diversity Index-Based Application for Detecting, Assessing and Monitoring Coastal Land-Cover/Land-Use Changes at High Spatial Resolution. *J. Coast. Res.* **2020**, *95*, 1315. [CrossRef]
26. Tassi, A.; Massetti, A.; Gil, A. The Spectralrao-Monitoring Python Package: A RAO's Q Diversity Index-Based Application for Land-Cover/Land-Use Change Detection in Multifunctional Agricultural Areas. *Comput. Electron. Agric.* **2022**, *196*, 106861. [CrossRef]
27. Michele, T.; Duccio, R.; Marc, Z.; Ruth, S.; Giustino, T. Testing the Spectral Variation Hypothesis by Using the RAO-Q Index to Estimate Forest Biodiversity: Effect of Spatial Resolution. In Proceedings of the IGARSS 2018—2018 IEEE International Geoscience and Remote Sensing Symposium, Valencia, Spain, 22–27 July 2018; IEEE: Piscataway, NJ, USA, 2018; pp. 1183–1186.
28. Liccari, F.; Sigura, M.; Bacaro, G. Use of Remote Sensing Techniques to Estimate Plant Diversity within Ecological Networks: A Worked Example. *Remote Sens.* **2022**, *14*, 4933. [CrossRef]
29. Rocchini, D.; Marcantonio, M.; Ricotta, C. Measuring Rao's Q Diversity Index from Remote Sensing: An Open Source Solution. *Ecol. Indic.* **2017**, *72*, 234–238. [CrossRef]
30. Khare, S.; Latifi, H.; Rossi, S. Forest Beta-Diversity Analysis by Remote Sensing: How Scale and Sensors Affect the Rao's Q Index. *Ecol. Indic.* **2019**, *106*, 105520. [CrossRef]
31. Rocchini, D.; Marcantonio, M.; Da Re, D.; Chirici, G.; Galluzzi, M.; Lenoir, J.; Ricotta, C.; Torresani, M.; Ziv, G. Time-Lapsing Biodiversity: An Open Source Method for Measuring Diversity Changes by Remote Sensing. *Remote Sens. Environ.* **2019**, *231*, 111192. [CrossRef]
32. Jornal Oficial das Comunidades Europeias. European Commission Council Regulation (EEC) No 1973/92. *Off. J. Eur. Communities* **1992**, *35*, 1–6.
33. SPEA. *Priolo LIFE: Recuperação Do Habitat. Do Priolo Na Zpe Picoda Vara/Ribeira Do Guilherme*; Sociedade Portuguesa para o Estudo das Aves: Lisboa, Portugal, 2009.
34. SPEA. *Relatório Final Do Projeto LIFE+ Laurissilva Sustentável (LIFE07 ENV/P/000630)*; Sociedade Portuguesa para o Estudo das Aves: Lisboa, Portugal, 2013; pp. 3–56.
35. SPEA. *Relatório Final Do Projeto LIFE+ Terras Do Priolo—Proteção Ativa Da População Do Priolo e Seus Habitats e Gestão Sustentável Das ZPE Do Pico Da Vara/Ribeira Do Guilherme*; Sociedade Portuguesa para o Estudo das Aves: Lisboa, Portugal, 2020.
36. SPEA. *Plano Operacional Da Mata Dos Bispos, São Miguel—Versão 1.0 Projeto LIFE IP AZORES NATURA—Proteção Ativa e Gestão Integrada Da Rede Natura 2000 Nos Açores*; Azores: Nordeste, Portugal, 2020.

37. Botelho, R.; De la Cruz, A.; Figueiredo, F.; Costa, T.; Mendonça, A.; Amaral, A.; Marquez, B.; Teixeira, R. Priolo, Como a Conservação de Uma Espécie Pode Alterar a Gestão de Um Território.
38. de Costa, T.M.M.; Gil, A.; Timóteo, S.; Ceia, R.S.; Coelho, R.; de la Cruz Martin, A. How Many Azores Bullfinches (Pyrrhula Murina) Are There in the World? Case Study of a Threatened Species. *Diversity* **2023**, *15*, 685. [CrossRef]
39. Gil, A.; Fonseca, C.; Lobo, A.; Calado, H. Linking GMES Space Component to the Development of Land Policies in Outermost Regions—The Azores (Portugal) Case-Study. *Eur. J. Remote Sens.* **2012**, *45*, 263–281. [CrossRef]
40. Gorelick, N.; Hancher, M.; Dixon, M.; Ilyushchenko, S.; Thau, D.; Moore, R. Google Earth Engine: Planetary-Scale Geospatial Analysis for Everyone. *Remote Sens. Environ.* **2017**, *202*, 18–27. [CrossRef]
41. Kumar, L.; Mutanga, O. Google Earth EngineApplications Since Inception: Usage, Trends and Potential. *Remote Sens.* **2018**, *10*, 1509. [CrossRef]
42. Navarro, J. First Experiences with Google EarthEngine. In Proceedings of the 3rd International Conference on Geographical Information Systems Theory, Applications and Management, Porto, Portugal, 27–28 April 2017.
43. Beller, W.; Beller, W.S.; D'Ayala, P.G.; Hein, P. *Sustainable Development and Environmental Management of Small Islands*; UNESCO: Lancashire, UK, 1990; Volume 5.
44. Tucker, C.J. Red and Photographic Infrared Linear Combinations for Monitoring Vegetation. *Remote Sens. Environ.* **1979**, *8*, 127–150. [CrossRef]
45. Jena, J.; Misra, S.R.; Tripathi, K. Normalized Difference Vegetation Index (NDVI) and Its Role in Agriculture. *Agric. Food* **2019**, *1*, 387–389.
46. Tenreiro, T.R.; García-Vila, M.; Gómez, J.A.; Jiménez-Berni, J.A.; Fereres, E. Using NDVI for the Assessment of Canopy Cover in Agricultural Crops within Modelling Research. *Comput. Electron. Agric.* **2021**, *182*, 106038. [CrossRef]
47. Sruthi, S.; Aslam, M.A.M. Agricultural Drought Analysis Using the NDVI and Land Surface Temperature Data; a Case Study of Raichur District. *Aquat. Procedia* **2015**, *4*, 1258–1264. [CrossRef]
48. Matas-Granados, L.; Pizarro, M.; Cayuela, L.; Domingo, D.; Gómez, D.; García, M.B. Long-Term Monitoring of NDVI Changes by Remote Sensing to Assess the Vulnerability of Threatened Plants. *Biol. Conserv.* **2022**, *265*, 109428. [CrossRef]
49. Skarlatos, D.; Vlachos, M. Vegetation Removal from UAV Derived DSMS, Using Combination of RGB and NIR Imagery. *Remote Sens. Spat. Inf. Sci.* **2018**, *IV-2*, 255–262. [CrossRef]
50. Roy, B. Asssment of Vegetation Health in Saint Martins Island, Bangladesh Using Remote Sensing and GIS. *Int. J. Innov. Eng. Res. Technol.* **2020**, *7*, 87–89. [CrossRef]
51. Thouverai, E.; Marcantonio, M.; Bacaro, G.; Da Re, D.; Iannacito, M.; Marchetto, E.; Ricotta, C.; Tattoni, C.; Vicario, S.; Rocchini, D. Measuring Diversity from Space: A Global View of the Free and Open Source Rasterdiv R Package under a Coding Perspective. *Community Ecol.* **2021**, *22*, 1–11. [CrossRef]
52. Lillesand, T.M.; Kiefer, R.W. *Remote Sensing and Image Interpretation*; John Wiley & Sons: Hoboken, NJ, USA, 2000; Volume 736.
53. Shivakumar, R.; Rajashekararadhya, S. An Investigation on Land Cover Mapping Capability of Classical and Fuzzy Based Maximum Likelihood Classifiers. *Int. J. Eng. Technol.* **2018**, *7*, 939. [CrossRef]
54. Richards, J.A. (Ed.) *Remote Sensing Digital Image Analysis*, 5th ed.; Springer: Berlin/Heidelberg, Germany, 2013; 494p, ISBN 978-3-642-30061-5.
55. Okwuashi, O.; Isong, M.; Eyo, E.; Eyoh, A.; Nwanekezie, O.; Olayinka, D.N.; Udoudo, D.O.; Ofem, B. GIS Cellular Automata Using Artificial Neural Network for Land Use Change Simulation of Lagos, Nigeria. *J. Geogr. Geol.* **2012**, *4*, 94–101. [CrossRef]
56. SPEA. *Recuperação Do Habitat Do Priolo Na ZPE Pico Da Vara/Ribeira Do Guilherme. LIFE 03NAT/P/000013. Relatório Final*; SPEA: Lisboa, Portugal, 2009.
57. Motohka, T.; Nasahara, K.N.; Oguma, H.; Tsuchida, S. Applicability of Green-Red Vegetation Index for Remote Sensing of Vegetation Phenology. *Remote Sens.* **2010**, *2*, 2369–2387. [CrossRef]
58. Cimtay, Y.; Ozbay, B.; Yilmaz, G.N.; Bozdemir, E. A New Vegetation Index in Short-Wave Infrared Region of Electromagnetic Spectrum. *IEEE Access* **2021**, *9*, 148535–148545. [CrossRef]
59. Mayer, R.R.; Scribner, D.A. *Extending the Normalized Difference Vegetation Index (NDVI) to Short-Wave Infrared Radiation (SWIR) (1- to 2.5-Mm)*; Shen, S.S., Ed.; SPIE: Bellingham, DC, USA, 2002; p. 182.